

Intrinsic electric quadrupole moment of the $K^\pi = 8^-$ isomeric state in ^{178}Hf

S. Zhu 

National Nuclear Data Center, Brookhaven National Laboratory, Upton, New York 11973, USA
and Physics Division, Argonne National Laboratory, Argonne, Illinois 60439, USA



(Received 28 May 2020; accepted 12 October 2020; published 26 October 2020)

The lifetime of the 9^- state in the rotational band based on the 4.0 s, $K^\pi = 8^-$, isomeric state ($^{178}\text{Hf}^{m_1}$) from the decay of the 31-yr isomer ($^{178}\text{Hf}^{m_2}$) was determined to be 99(2) ps by means of the fast-timing technique using two $\text{LaBr}_3(\text{Ce})$ scintillators. The $\delta(E2/M1)$ mixing ratios of the $\Delta I = 1$ γ rays depopulating levels in this band were deduced from γ - γ angular correlations by using a $^{178}\text{Hf}^{m_2}$ radioactive source located at the center of the Gammasphere HPGe detector array. The new results, together with previous spectroscopic information, provide a different way to extract the intrinsic quadrupole moment of $Q_0 = 6.45(14)$ eb for the $^{178}\text{Hf}^{m_1}$ band. A possible explanation for the reduction of the $^{178}\text{Hf}^{m_1}$ nuclear charge radius is presented.

DOI: [10.1103/PhysRevC.102.044326](https://doi.org/10.1103/PhysRevC.102.044326)

I. INTRODUCTION

The decay of the 31-yr, $K^\pi = 16^+$ isomer $^{178}\text{Hf}^{m_2}$ (Fig. 1) has been extensively studied in the past [1]. It is known to proceed via a rotational band built on the 4.0 s, $K^\pi = 8^-$ isomeric state ($^{178}\text{Hf}^{m_1}$). This situation is ideal, not only for probing the configuration of the isomeric state directly, but also for determining its properties independently by inspecting the characteristics of the states in the band. The level energies in this sequence and the corresponding γ -ray transition intensities have been measured well [1], but additional information, including the lifetimes of these collective states, and the mixing ratios of the depopulating γ rays, is required to deduce collective transition strengths, from which the intrinsic quadrupole moment Q_0 can be determined. Collinear laser spectroscopy experiments have been performed to measure the spectroscopic electric-quadrupole (Q_s) and magnetic-dipole moments (μ) of the 8^- and 16^+ isomers [2,3]. These studies revealed that the mean-square charge radii $\langle r^2 \rangle$ of both isomers are smaller than that of the ground state, despite the increase of their intrinsic electric-quadrupole moments (Q_0) [2,3]. This observation is in contrast with the general expectations that a smaller $\langle r^2 \rangle$ value in a nucleus is associated with a smaller Q_0 moment. To date, this anomalous phenomenon has been observed only for a few multiquasiparticle isomeric states besides $^{178m_{1,2}}\text{Hf}$ [3–8].

It has been argued that this effect was most probably caused by an increase in nuclear rigidity or a decrease in nuclear surface diffuseness for the multiquasiparticle state [3,9] under consideration, related to weaker pairing resulting from the blocking of broken nucleon pairs [10]. It should be noted that, in the case of an even-even nucleus such as ^{178}Hf , the Q_0 value of the ground state was deduced from the $B(E2)$ strength of the 2^+ level. This represents a measure in the intrinsic coordinate system. In contrast, for the isomers, it

was calculated from Q_s moments obtained using the collinear laser spectroscopic method, e.g., from expectation values in the laboratory system. In Ref. [3], it was argued that Q_s is only sensitive to the static quadrupole shape, but that the $B(E2)$ strength reflects the total, dynamic, and static deformation. To put the comparison on the same footing, it is desirable to accurately obtain the Q_0 value in the $^{178}\text{Hf}^{m_1}$ band by measuring the $B(E2; 9^- \rightarrow 8^-)$ transition probability.

Obtaining $B(E2)$ values usually involves measuring sub-nanosecond lifetimes. In general, the commonly utilized techniques, such as the Doppler-shift attenuation method or multistep Coulomb excitation provide a value averaged over the entire band with a systematic uncertainty often around 5%. However, it is technically challenging to achieve the goal of determining them individually for each state in a particular rotational sequence. Recent progress in γ -ray fast-timing detection using $\text{LaBr}_3(\text{Ce})$ scintillators has resulted in much improved lifetime measurements of nuclear states down to tens of picoseconds [11,12]. The estimated lifetime of the 9^- state is in a range achievable by such detectors. The γ -ray $E2/M1$ mixing ratios of the $\Delta I = 1$ transitions within the $K^\pi = 8^-$ band have been deduced in the past from conversion electron data [13] and from a γ - γ angular correlation analysis [14]. The results of both methods are in overall agreement with each other, but suffer from rather large uncertainties, due to poor counting efficiency and sensitivity for the detection setup involved. The high-efficiency, multidetector array Gammasphere [15] offers an opportunity for a mixing ratio determination with higher accuracy. This article reports on a new examination of the decay of $^{178}\text{Hf}^{m_2}$, with a focus on quantifying the properties of the states belonging to the $K^\pi = 8^-$, $^{178}\text{Hf}^{m_1}$ band.

II. EXPERIMENT

Several measurements were performed at Argonne National Laboratory. For the lifetime measurements, a radioactive $^{178}\text{Hf}^{m_2}$ source was placed about 1 inch away from two

* shaofei@bnl.gov

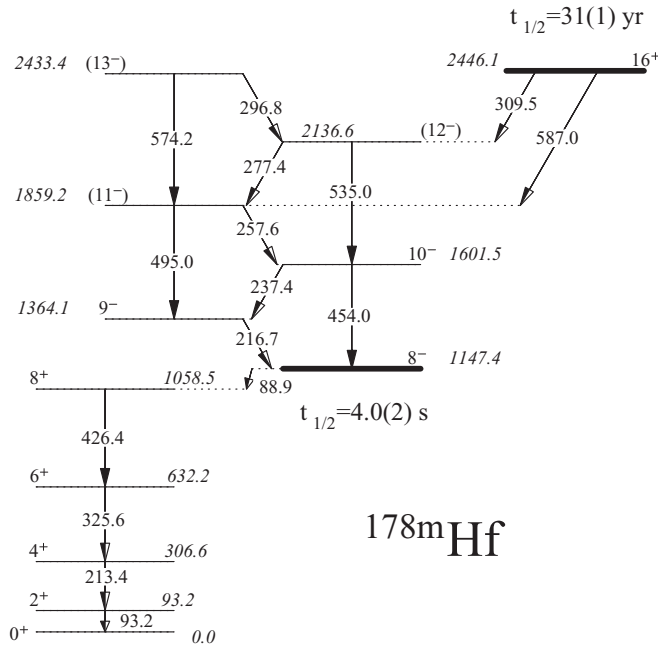


FIG. 1. Partial decay scheme of $^{178m_2}\text{Hf}$ from Ref. [1].

LaBr₃(Ce) scintillator detectors located in opposite directions, while facing each other. The crystals were 1 inch by 1 inch in size and of a cylindrical shape; this is suitable for fast-timing measurements. Most of the transitions from the isomer decay can be resolved in the scintillator spectrum, as seen in Fig. 2(a). However, the 89- and 93-keV γ rays from the same prompt cascade lie too close in energy to be resolved by these scintillators. Hence, in order to isolate the cascade of

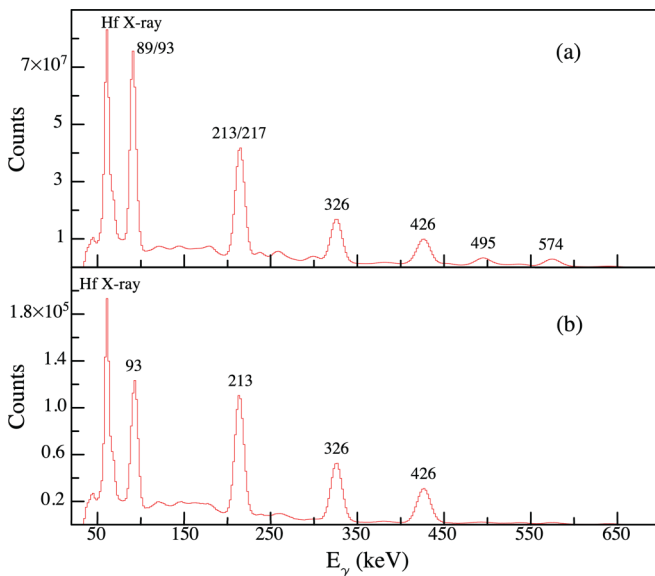


FIG. 2. (a) Singles γ -ray spectrum obtained by the LaBr₃(Ce) detectors. (b) Spectrum from the LaBr₃(Ce) detectors after requiring a coincidence with the 89-keV transition observed in the HPGe detectors. Note that no Compton background subtraction was applied to the gating procedure on the HPGe detectors.

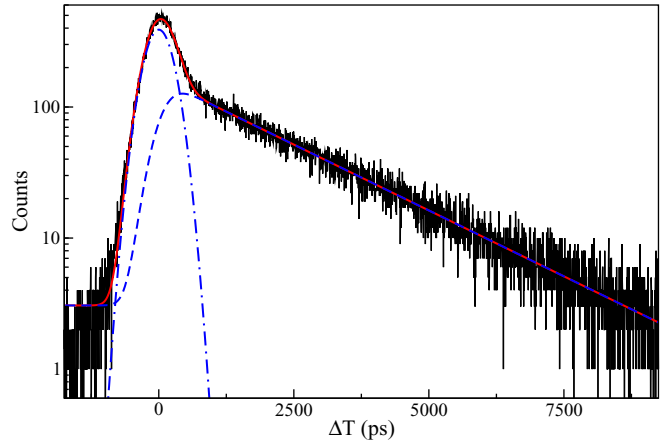


FIG. 3. Timing spectra measured by the two LaBr₃(Ce) detectors between the 213- and 93-keV transitions after gating on the 89-keV γ ray in the clover HPGe detector. The red solid line is the results of the fit comprising the blue, short-dashed line corresponding to the convoluted exponential and Gaussian component, and the blue dot-dashed line to the prompt Gaussian component. See text for details [$\sigma = 252(12)$ ps, $\tau = 2160(30)$ ps, $\chi^2/\text{nof} = 1.27$].

213- and 93-keV γ rays in the LaBr₃(Ce) spectra for an accurate lifetime measurement of the 2^+ state, these detectors were coupled to a clover HPGe detector, and the data acquisition (DAQ) was enabled by an event where both scintillators fired within 50 ns of each other, with or without the presence of a signal from the HPGe detectors. With this arrangement, coincidence gates placed on the high-resolution clover spectra contribute to the appropriate selection of the transitions of interest in the LaBr spectra. In Fig. 2(b), a coincidence spectrum gated on the 89-keV transition in the HPGe detectors illustrates the quality of the resulting spectrum by displaying clearly the transitions in the ground-state band populated by the $4s$ isomer. The DAQ also included two time-to-amplitude converters (TAC), where the trigger provided the stop signal, and signals from the respective scintillators were used as starts. Time-difference spectra between the γ ray feeding the state and the one depopulating it were produced from the TAC between the two LaBr₃(Ce) detectors. Even with a short lifetime in the range of ≈ 1 ns, the slope of the TAC spectrum is well defined, as demonstrated in Fig. 3.

The TAC spectrum was evaluated by using an exponential decay convoluted with a Gaussian distribution in addition to another Gaussian constrained to the same σ (the standard deviation) as those in the convolution. A constant background was also included as a free parameter in the fit. In this expression, $\text{exponential} * \text{gaussian}_1 + \text{gaussian}_2 + \text{background}$, the second term, gaussian_2 , was attributed to the prompt component and originates from the Compton-scattered γ rays from higher-energy transitions partially depositing their energies in the scintillators. The second Gaussian term was introduced in the fitting to avoid additional uncertainties by applying Compton background subtraction. Because the σ value is required to be the same for the first and second term, gaussian_2 also served as the coherently fit prompt response function for the setup. The validity of this

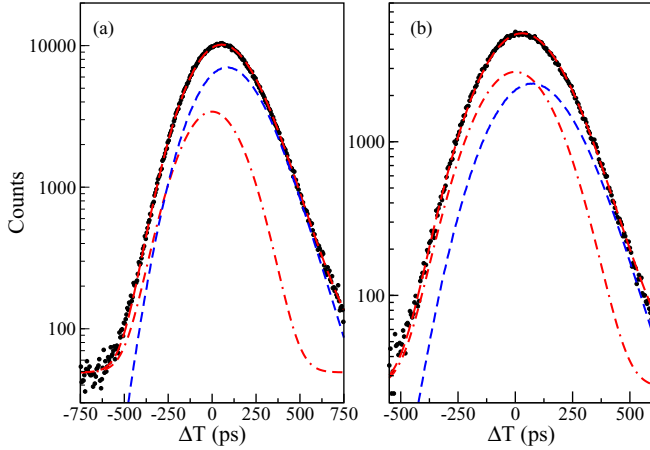


FIG. 4. (a) Timing spectra measured by the two LaBr₃(Ce) detectors between the 326- and 213-keV transitions [$\sigma = 157(1)$ ps, $\tau = 120(3)$ ps, $\chi^2/\text{nof} = 1.31$]. (b) Timing spectra between the 495- and 217-keV transitions [$\sigma = 150(1)$ ps, $\tau = 99(2)$ ps, $\chi^2/\text{nof} = 1.50$]. The red long-dashed lines are the result of the fitting, while the blue short-dashed lines are the convoluted exponential and Gaussian component, and the red dot-dashed lines are the prompt Gaussian component.

approach in this specific application was checked by considering the 9^- state. The fitted σ value [151(1) ps] of the TAC spectrum between the 495- and 217-keV transitions (Fig. 4), is consistent with the prompt σ value [145(1) ps] obtained from the time distribution between the 495-keV γ ray and the Compton background region extending from 237 to 255 keV when the dependence of the timing resolution on the γ -ray energy is considered.

The lifetime of the 2^+ level of the ground-state band was determined to be 2160(30) picoseconds from the fit of the time spectrum in Fig. 3. This value is consistent with the adopted one of 2155(33) ps, see Ref. [1]. The lifetime of the 4^+ state was measured to be 120(3) ps with an accuracy comparable to that of the 2^+ level [Fig. 4(a)]. The 9^- state in the $^{178}\text{Hf}^{m_1}$ band at 1364 keV has a lifetime 99(2) ps, as seen in Fig. 4(b).

Measurement of angular correlations was performed by placing the same ^{178}Hf isomeric source in the center of Gammasphere. The angles between pairs of detectors in Gammasphere were deduced from the well-established positions in θ and ϕ of each detector. The angular correlation can be expressed as $W(\theta) = A_0(1 + Q_2A_2P_2\cos\theta + Q_4A_4P_4\cos\theta)$ [16], where A_2 and A_4 describe the multipolarity of the observed γ rays, Q_2 and Q_4 are the solid-angle correction factors, and $P_2(\cos\theta)$ and $P_4(\cos\theta)$ are the Legendre polynomials. The Q_2 and Q_4 factors for each detector are considered to be unity in this instance, as all detectors are axially symmetric about the γ -ray propagation direction and are irradiated from a source located in the center of Gammasphere, roughly 25 cm away. As a result, the form of the angular-correlation function is unchanged, which is justified by the comparison between the measured angular-correlation coefficients for the 426–326-keV cascade [$A_2 = 0.1021(8)$, $A_4 = 0.0088(10)$] and the theoretical value for an $8^+6^+-4^+$ sequence ($A_2 =$

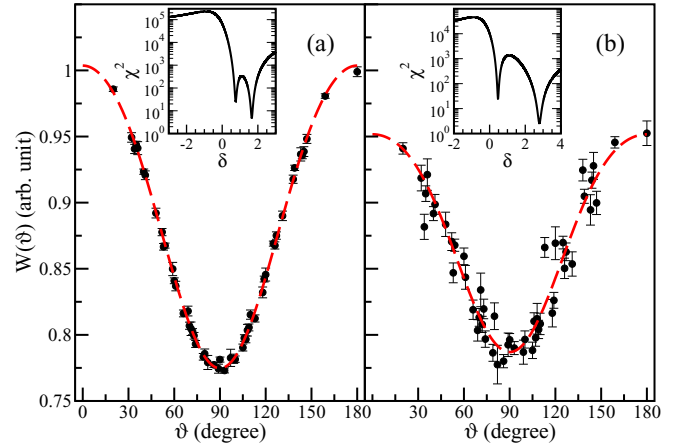


FIG. 5. Angular correlations for (a) the 495–217-keV cascade and (b) the 535–237-keV cascade. Red dashed lines correspond to the fit function, while the inset panels are associated with the calculated χ^2 between theoretical and experimental A_2 and A_4 coefficients as a function of mixing ratio δ used to determine the δ value from the χ^2 minimization.

0.1020, $A_4 = 0.0091$). The quality of data is demonstrated in Fig. 5.

In the angular-correlation analysis, one of the γ rays in the cascade was selected to correspond to a known $E2$ transition. Consequently, the values of the correlation coefficients A_2 and A_4 only depend on the mixing ratio $\delta(E2/M1)$ of the other coincident γ ray. For instance, as shown in Fig. 5(a), the coefficients were obtained as $A_2 = 0.1846(10)$ and $A_4 = -0.0169(14)$ for the 495–217-keV cascade, establishing a mixing ratio value $\delta = 1.66(2)$ for the 217-keV γ ray. The results of the angular-correlation measurements are listed in Table I for the $\Delta I = 1$ transitions involved in the rotational band of $^{178}\text{Hf}^{m_1}$. Two χ^2 minima exist as a general feature for mixing-ratio determination. The listed results corresponded to the smallest minimum, which is about a factor of ten lower than the other one in all cases.

III. RESULTS

The Q_0 values of the three states were deduced from the measured lifetimes based on the fact that ^{178}Hf is an axially symmetric rigid rotor with the condition $Q_{22} = Q_{21}$, using

$$Q_0^2 = \frac{16\pi}{5} \frac{B(E2, I_i \rightarrow I_f)}{\langle I_i K 2 0 | I_f K \rangle^2}. \quad (1)$$

Here, $B(E2)$ is the reduced $E2$ γ -ray transition probability from the initial $(I_i K)$ state to the final $(I_f K)$ state [Eq. (2)], and $\langle I_i K 2 0 | I_f K \rangle$ is the associated Clebsch-Gordan coefficient. Thus,

$$B(E2, I_i \rightarrow I_f) = \frac{0.08164}{\tau(E2)(1 + \alpha_{\text{tot}})E_\gamma^5}, \quad (2)$$

where $\tau(E2)$ (in ps) is the mean lifetime of the $E2$ transition with energy E_γ in MeV, and α_{tot} is the total conversion electron coefficient. In the case of the 9^- level, $\tau(E2)$ was determined to be 135(4) ps by combining its lifetime $\tau =$

TABLE I. The mixing ratios for the $\Delta I = 1$ transitions in the rotational band of $^{178}\text{Hf}^{m1}$.

I_i^π	I_f^π	E_γ [keV]	A_2	A_4	δ
9 ⁻	8 ⁻	217	0.1846(10)	-0.0169(14)	1.66(2)
10 ⁻	9 ⁻	237	0.130(2)	-0.020(3)	2.79(5)
11 ⁻	10 ⁻	258	0.027(1)	-0.026(1)	9.4(2)
12 ⁻	11 ⁻	277	-0.143(5)	-0.036(7)	-9.2(8)
13 ⁻	12 ⁻	297	-0.2409(14)	-0.0362(19)	-3.32(4)

99(2) ps and the mixing ratio $\delta = 1.66(2)$ of the $9^- \rightarrow 8^- \gamma$ transition.

The results of the deduced individual Q_0 values are summarized in Table II. The values for the 2^+ and 4^+ states are consistent with the value $Q_0 = 6.86(3)$ eb for the 6^+ through 18^+ states in the ground-state band determined from a multistep Coulomb excitation measurement [17]. In the case of the $K^\pi = 8^-$ band, no Q_0 results were available from this Coulomb excitation measurement of Ref. [17]. The value $Q_0 = 7.11(6)$ eb for the 8^- state was determined from the collinear laser spectroscopic result $Q_s = 4.99$ eb with the relation [3]

$$Q_0 = \frac{(I+1)(2I+3)}{I(2I-1)}Q_s. \quad (3)$$

This Q_0 value is 10(2)% larger than that for the 9^- state, $Q_0 = 6.45(14)$ eb, deduced from its lifetime.

Extensive studies on the $^{178}\text{Hf}^{m2}$ decay have shown that the $K^\pi = 8^-$ band is characterized by mixed two-quasiparticle configurations of $\nu 9/2^+[624] \otimes 7/2^- [514]$ and $\pi 9/2^- [514] \otimes 7/2^+ [404]$ [13,19,20], respectively. The $\frac{B(E2, I \rightarrow I-1)}{B(E2, I \rightarrow I-2)}$ ratios derived from the branching and mixing ratios are compared with calculated values of $\frac{(IK20I-1K)^2}{(IK20I-2K)^2}$ with $K = 8$ in Table III. Such a comparison clearly indicates that the quadrupole moment Q_0 in the band remains nearly constant, not influenced by the possible change of mixing ratio of the neutron and proton components. In particular, the 10(2)% reduction of the Q_0 values between the 9^- and 8^- states derived from two different methods is not a manifestation of the change in admixtures in the neutron and proton configurations.

IV. DISCUSSION

The collinear laser spectroscopic study of the $^{178m1}\text{Hf}$ [3] isomer has revealed that its mean-square charge radius $\langle r^2 \rangle$ is significantly smaller than that of the ground state, despite

TABLE II. Q_0 values from measured lifetimes $\tau(E2)$; the α_{tot} coefficients were calculated by using the BrIcc code [18] (within the frozen orbital approximation) based on γ -ray energies, assigned multipolarities, and mixing ratios.

I_i^π	I_f^π	K	E_γ [MeV]	$\tau(E2)$ [ps]	α_{tot}	Q_0 [eb]
2 ⁺	0 ⁺	0	0.09320(7)	2160(30)	4.74(1)	6.86(7)
4 ⁺	2 ⁺	0	0.2134378(21)	120(3)	0.234(5)	6.62(8)
9 ⁻	8 ⁻	8	0.216668(7)	135(4)	0.282(4)	6.45(14)

the fact that its quadrupole moment is larger. This effect appears to contradict the presumed firm relationship between the changes in radii and those in Q_0 moments. Besides this measurement, seven other cases also show the same effect, as summarized in Ref. [3]. The change of the $\langle r^2 \rangle$ values with respect to the change of the quadrupole deformation parameter β_2 is described as

$$\delta \langle r^2 \rangle = \frac{5}{4\pi} \langle r^2 \rangle_0 \delta \langle \beta_2^2 \rangle, \quad (4)$$

in which $\langle \beta_2^2 \rangle = \langle \beta_2 \rangle^2 + (\langle \beta_2^2 \rangle - \langle \beta_2 \rangle^2)$ is a sum of the static deformation $\langle \beta_2 \rangle^2$ and the deformation $\langle \beta_2^2 \rangle - \langle \beta_2 \rangle^2$ arising from the zero-point fluctuations of the nuclear surface. Here $\langle r^2 \rangle_0$ is the mean-square radius of a spherical nucleus of the same volume. Because Q_s only reflects the static deformation $\langle \beta_2 \rangle$, and Q_0 , derived from the $B(E2)$ strength, measures the total deformation $\langle \beta_2^2 \rangle^{1/2}$, which is directly related to $\langle r^2 \rangle$, it is even more surprising to observe a smaller $\langle r^2 \rangle$ value seemingly associated with a larger static deformation $\langle \beta_2 \rangle$ for the isomeric state.

This surprising observation has been attributed either to a decrease in diffuseness of the nuclear surface or to an increase in nuclear rigidity for a multi-quasiparticle state [3,9]. It has been pointed out in Ref. [26] that the deformation part of $\delta \langle r^2 \rangle$ remains unchanged when the diffuseness of the nuclear surface is described by folding a sharp-edged distribution with a Gaussian one. The nuclear rigidity effects could possibly be related to the derivation of the Q_0 quadrupole moment. The relation between Q_0 and Q_s defined by Eq. (3) is expected to be valid in the limit of a well-deformed, rigid rotor with the assumptions that the relation $\langle \beta_2^2 \rangle = \langle \beta_2 \rangle^2$ applies and that the strong coupling rule is reliable. In the $K^\pi = 8^-$ band, when comparing the Q_0 value based on the Q_s measurement of the 8^- state, with that determined from the lifetime

TABLE III. The $\frac{B(E2, I \rightarrow I-1)}{B(E2, I \rightarrow I-2)}$ ratios derived from the branching and mixing ratios, and calculated values of $\frac{(IK20I-1K)^2}{(IK20I-2K)^2}$ with $K = 8$, for states I^π in the rotational band of $^{178}\text{Hf}^{m1}$. The experimental γ -ray branching ratios are the weighted average of results from Refs. [13,21–25], and the mixing ratios are from this work.

I^π	$\frac{B(E2, I \rightarrow I-1)}{B(E2, I \rightarrow I-2)}_{\text{expt}}$	$\frac{(IK20I-1K)^2}{(IK20I-2K)^2}$
10 ⁻	12.7(3)	13.0
11 ⁻	6.1(2)	6.2
12 ⁻	3.8(5)	4.0
13 ⁻	2.76(5)	2.86

measurement for the 9^- state, a 10% lowering is apparent. This lower value indicates the inadequacy of Eq. (3). In addition, it is also lower than that obtained for the ^{178}Hf ground-state band, based on the $B(E2)$ measurements, in agreement with a negative $\delta\langle r^2 \rangle_{g.m.}^{s.m.}$ value for the change of $\langle r^2 \rangle$ from the ground state to the $^{178}\text{Hf}^{m_1}$ isomeric state reported in Ref. [3]. These arguments provide a plausible indication that deducing Q_0 from Q_s is not as accurate as expected *a priori*. In turn, this is an indication that the nuclear deformation is not as rigid as generally thought, even in $^{178m_1}\text{Hf}$, although this is in distinctive contrast with the expectation that the isomeric band should be more rigid due to blocking effects from the unpaired quasiparticles. Note that the extraction of Q_0 values from the measured lifetimes was based on the rigid-rotor model with the assumption that nuclear deformation is independent of angular momentum, i.e., without taking into account higher-order effects in the deformation. In addition, only changes in $\langle r^2 \rangle$ can be determined from laser spectroscopy, while nonoptical, absolute measurements of $\langle r^2 \rangle$ are directly associated with the absolute $\langle \beta^2 \rangle$ deformation. Therefore, an accurate description of the measured $\delta\langle r^2 \rangle$ value involving multi-quasiparticle isomeric states remains entangled.

Discussions on the origin of nuclear softness in well-deformed nuclei with large quadrupole deformation can be found in the literature. Systematic theoretical investigations of $K^\pi = 8^-$ isomeric states have revealed strong shape polarization effects caused by two-quasiparticle configurations, emphasizing particularly the involvement of the $\nu i_{13/2}$ and $\pi h_{9/2}$ orbitals [27]. The evolution of quadrupole moments

with increasing spin is possibly associated with polarization effects caused by particle alignments. In addition, the moments of inertia of rotational sequences in well-deformed nuclei display apparent inconsistencies with expectations based on a rotating rigid-body. Such inconsistencies have been observed and calculated systematically for high- K rotational bands in ^{178}Hf , ^{178}W , and ^{179}W [28].

V. CONCLUSIONS

The intrinsic electric-quadrupole moment Q_0 for the $K^\pi = 8^-$ band was determined from the lifetime of the 9^- state. This approach provides an alternative way to compare the Q_0 moments of the ground state and $K^\pi = 8^-$ bands, which indicates that the reduction of the mean-square charge radius of $^{178}\text{Hf}^{m_1}$ is consistent with the change in Q_0 value deduced from lifetimes. It also indicates that the relation between the intrinsic quadrupole moments Q_0 and the spectroscopic quadrupole one Q_s can be described by Eq. (3) but with at most 10% accuracy, even in the case of a well-deformed axially symmetric nucleus.

ACKNOWLEDGMENTS

This material is based upon work supported by the U.S. Department of Energy, Office of Science, Office of Nuclear Physics, under Contracts No. DE-AC02-98CH10886 (BNL) and No. DE-AC02-06CH11357 (ANL). This research used resources of the ANL's ATLAS facility, which is a DOE Office of Science User Facility.

-
- [1] E. Achterberg, O. A. Capurro, and G. V. Marti, *Nucl. Data Sheets* **110**, 1473 (2009).
- [2] N. Boos *et al.*, *Phys. Rev. Lett.* **72**, 2689 (1994).
- [3] M. L. Bissell *et al.*, *Phys. Lett. B* **645**, 330 (2007).
- [4] C. Thibault *et al.*, *Nucl. Phys. A* **367**, 1 (1981).
- [5] R. C. Thompson *et al.*, *J. Phys. G: Nucl. Phys.* **9**, 443 (1983).
- [6] U. Georg *et al.*, *Eur. Phys. J. A* **3**, 225 (1998).
- [7] R. Moore *et al.*, *Phys. Lett. B* **547**, 200 (2002).
- [8] B. Cheal *et al.*, *Phys. Lett. B* **645**, 133 (2007).
- [9] Y. Gangrsky, *Hyperfine Interact.* **171**, 203 (2006).
- [10] N. Pillet, P. Quentin, and J. Libert, *Nucl. Phys. A* **697**, 141 (2002).
- [11] N. Mărginean *et al.*, *Eur. Phys. J. A* **46**, 329 (2010).
- [12] S. Zhu *et al.*, *Nucl. Instrum. Methods Phys. Res. Sect. A* **652**, 231 (2011).
- [13] F. W. N. De Boer, P. F. A. Goudsmit, B. J. Meijer, J. C. Kapteyn, J. Konijn, and R. Kamermans, *Nucl. Phys. A* **263**, 397 (1976).
- [14] P. Tlustý, D. Vénos, A. Kugler, M. Honusek, and B. Gorski, *Phys. Rev. C* **48**, 2082 (1993).
- [15] I.-Y. Lee, *Nucl. Phys. A* **520**, c641 (1990).
- [16] R. M. Steffen and K. Alder, in *The Electromagnetic Interaction in Nuclear Physics*, edited by W. D. Hamilton (North-Holland, Amsterdam, 1973).
- [17] A. B. Hayes *et al.*, *Phys. Rev. C* **75**, 034308 (2007).
- [18] T. Kibédi, T. W. Burrows, M. B. Trzhaskovskaya, P. M. Davidson, and C. W. Nestor, Jr., *Nucl. Instrum. Methods Phys. Res., Sect. A* **589**, 202 (2008).
- [19] R. G. Helmer and C. W. Reich, *Nucl. Phys. A* **211**, 1 (1973).
- [20] T. L. Khoo and G. Løvholden, *Phys. Lett. B* **67**, 271 (1977).
- [21] R. G. Helmer and C. W. Reich, *Nucl. Phys. A* **114**, 649 (1968).
- [22] J. Van Klinken, W. Z. Venema, R. V. F. Janssens, and G. T. Emery, *Nucl. Phys. A* **339**, 189 (1980).
- [23] W. Z. Venema, R. V. F. Janssens, J. Van Klinken, and G. T. Emery, *Nucl. Instrum. Methods Phys. Res.* **201**, 531 (1982).
- [24] J. B. Kim, J. Morel, M. Etcheverry, N. Coursoi, D. Trubert, O. Constantinescu, S. A. Karamian, Y. T. Oganessian, C. Briancon, and M. Hussonnois, *J. Radioanal. Nucl. Chem.* **215**, 229 (1980).
- [25] M. B. Smith, P. M. Walker, G. C. Ball, J. J. Carroll, P. E. Garrett, G. Hackman, R. Propri, F. Sarazin, and H. C. Scraggs, *Phys. Rev. C* **68**, 031302(R) (2003).
- [26] E. W. Otten, in *Treatise on Heavy-Ion Science*, edited by D. A. Bromley (Plenum Press, New York, 1989), Vol. 8, p. 570.
- [27] F. R. Xu, P. M. Walker, and R. Wyss, *Phys. Rev. C* **59**, 731 (1999).
- [28] S. Frauendorf, K. Neergard, J. A. Sheikh, and P. M. Walker, *Phys. Rev. C* **61**, 064324 (2000).